Thin Solid Films, 207 (1992) 90–97

The effects of mobility coalescence on the evolution of surface atomic clusters

M. Vicanek* and N. M. Ghoniem

Mechanical, Aerospace and Nuclear Engineering Department, University of California, Los Angeles, CA 90024-1597 (U.S.A.)

(Received October 23, 1990; revised April 16, 1991; accepted June 26, 1991)

Abstract

A numerical study of the effects of cluster mobility on the clustering kinetics during deposition of atoms on a substrate surface is presented. The pertinent rate equations are solved by a two-group approach of using discrete equations for small clusters and moment equations for large ones. The study is restricted to systems where the critical nucleus is a monomer (*e.g.* Ag/NaCl at low temperatures). It is shown that if small clusters are fairly mobile their population will quickly be depleted, resulting in an overall reduction of the total cluster density. Cluster mobility coalescence reduces the concentration and increases the growth of surface atomic clusters. The effects of cluster mobility coalescence are analyzed in terms of two mobility models: (1) where only small clusters, here up to dimers, are mobile, and (2) where all clusters are mobile with a diffusion coefficient given by size power law. Results of the analysis are presented for the total density of surface atomic clusters and their size distributions.

1. Introduction

The evolution of atomic clusters in the early stages of thin film formation by thermal atom deposition is an important phenomenon for a fundamental understanding of atomic clustering physics and for practical applications. Typical applications are encountered in chemical- and physical-vapor-deposition technologies. Classical nucleation theories [1–3] assume that single atoms deposited on the substrate surface exhibit diffusive motion until they either evaporate or collide with other adatoms or clusters and are captured. Clusters formed in this manner are often assumed to be immobile as a first approximation. However, there is experimental evidence for cluster mobility [4, 5] that is expected to affect the nucleation kinetics [6] by increasing the possibility for additional aggregation and coalescence events. Mobility coalescence is usually taken into account only in a somewhat general manner [6], or is considered merely as a perturbation [7]. In some cases [1, 8], however, specific calculations have been undertaken. A more refined treatment of mobility coalescence [8], however does not aim at calculating its effects on the size distribution.

Experimental evidence for cluster mobility suggest that isolated atomic islands on a substrate exhibit rotation and translation. Bassett [9, 10] evaporated silver, gold and copper onto substrates of MoS_2, graphite and amorphous carbon. He observed the nucleation, growth and coalescence processes under the electron microscope. Clusters as large as 50–100 Å were observed to move suddenly and coalesce with others. Growth sequences observed in the electron microscope by Poppa [11] also showed evidence of cluster mobility. Despite the argument that electrostatic effects might have caused such movements [12], further experimental evidence of cluster motion obtained without using the electron microscope were presented by Bachmann *et al.* [13], and by Skofronick and Philips 1[4]. However, their conclusions are based upon a decrease in the cluster density with deposition time, and on distortions of the cluster size distribution. These experimental inferences are indirect and, therefore, must be analyzed in terms of a detailed atomic-clustering model. Other direct observations of cluster mobility have been presented in the literature [15–18]. For example, Schwabe and Hayek [16] used the method of high resolution shadowing with tantalum/tungsten to study the surface migration of gold on vacuum-cleaved surfaces of NaCl and KCl under high and ultrahigh vacuum conditions.

In this article we view the problem of surface cluster evolution as an aggregation phenomenon where particles of any size may interact according to a given, size-dependent rate constant. Such systems are described by Smoluchowski's equation [19] and have been known in various different areas of research, as for instance aerosol physics [20] or star cluster physics [21]. Within this framework, we present a systematic study of the effects of

*Permanent address: Institute for Theoretical Physics, Technical University, PO Box 3329, W-3300 Braunschweig, F.R.G.

0040-6090/92/$5.00

mobility coalescence on the clustering kinetics, the evolution of individual clusters, and the size distribution. The present model is restricted to atomic deposition conditions where the critical nucleus size is only a monomer. This, for example, may apply to systems where the binding energy of dimers is large enough that dissociation is negligible (as in low temperature experiments of Ag/NaCl).

In Section 2, we present a kinetic model which includes mobility coalescence events, that describes the evolution of surface atomic clusters. In Section 3, we discuss mobility coalescence and give two models representing coalescence rates. Results of calculations of cluster densities and size distributions using our previously developed two-group moments method are given in Section 4. Conclusions drawn from this work are finally outlined in section 5.

2. Cluster evolution

Consider a system of atomic clusters on a structureless surface. Each cluster is supposed to have, to some degree, the capability to exhibit Brownian motion on the surface. This gives rise to collisions where two clusters may combine to form one large cluster containing the sum of the atoms of the two colliding clusters.

Let the number of clusters per unit area containing i atoms be $C_i(t)$, where t denotes the time. The rate of coalescence of an i-sized cluster with a j-sized cluster is given by $K(i,j)C_iC_j$, where $K(i,j)$ is a coalescence rate constant. Balancing all possible gain and loss processes, one obtains Smoluchowski's well-known equation [19, 22]

$$\frac{\partial}{\partial t}C_i = \frac{1}{2}\sum_{j=1}^{i-1} K(j,i-j)C_jC_{i-j} - \sum_{j=1}^{\infty} K(i,j)C_iC_j \quad i \geqslant 2 \quad (1)$$

Equation (1) describes an irreversible process. In some systems, clusters are not entirely stable but may dissociate spontaneously into fragments. Such a process may be included by adding appropriate terms [23, 24] to eqn. (1), but will be left out here. As mentioned earlier, we treat the case where dissociation of dimers and larger clusters is negligible (*i.e.* $i = 1$ systems).

For applications to surface atomic clustering during the early stages of thin film formation, two important processes have to be included, namely the deposition and evaporation of species. In most cases, this concerns only the monomers for which we get the equation

$$\frac{\partial}{\partial t}C_1 = -\sum_{j=1}^{\infty} K(1,j)C_1C_j - \frac{C_1}{\tau} + Q \quad (2)$$

where τ is the mean residence time of an adatom before evaporation and Q is the deposition rate of monomers per unit area.

Equations (1) and (2) describe the system considered here. Apart from the deposition and evaporation rates, all of the physics is contained in the coalescence rate constant, $K(i,j)$, particularly its dependence on the sizes of the coalescing clusters i and j. Other possible processes such as cluster growth by direct impingment [2] or nucleation at preferred sites [25] are excluded here so that we can focus on mobility coalescence effects. We have included such mechanisms in a separate publication [26] with the intention that the effects of each individual mechanism will be investigated without the added complexity of the simultaneity of processes which could make the interpretation of results somewhat ambiguous.

The system of eqns. (1) and (2) is theoretically an infinite set of nonlinear, ordinary differential equations. A solution method has been developed by us in a separate publication [24], and will be discussed briefly in Section 4.

3. Coalescence rates

In eqn. (1), the coalescence rate constant $K(i,j)$ appears as a phenomenological coefficient whose value may, in principle, be obtained from an appropriate microscopic theory. In thin film formation, two mechanisms leading to coalescence (*i.e.* migration and growth) are distinguished. Growth coalescence occurs typically at high surface coverage. In this paper, we wish to investigate mobility effects only; hence, we confine ourselves to low coverage (*e.g.* up to about 0.1 to 0.2 monolayers).

It is important to note that in diffusion-controlled reactions in two or less dimensions, the rate "constants" may actually depend on the concentrations of the reacting species [27]. Models for $K(i,j)$ based on diffusion theory have been developed for monomer capture by immobile clusters [2, 28, 29]. Here, one writes

$$K(1,i) = \sigma_i D_1 \quad (3)$$

where D_1 is the monomer diffusion coefficient and σ_i is a dimensionless quantity called the capture number. Equation (3) may be generalized [22] for collisions between two mobile clusters,

$$K(i,j) = \sigma_{ij}(D_i + D_j) \quad (4)$$

where σ_{ij} is a generalized capture number and $D_i + D_j$ is the diffusion coefficient for the relative motion of the two clusters.

3.1. Capture numbers

Consider first the capture of adatoms by immobile clusters (eqn. (3)). Diffusion calculations show that σ_i is not only dependent on the size i of the capturing cluster but is also determined by competing effects such as evaporation and capture by other clusters [29].

One limiting case, typically encountered at low

substrate temperatures, arises when an adatom is more likely to be captured by other clusters than to evaporate. For this capture-controlled case, the capture number is given by [30],

$$\sigma_i = 2\pi/\ln(R/r_i) \tag{5}$$

where r_i is the radius of an i-sized cluster and R is a length of the order of the average distance of two neighboring clusters:

$$R = \left(\pi \sum_{i=1}^{\infty} C_i\right)^{-1/2} \tag{6}$$

Equation (5) is valid for low fractional coverage

$$Z = \sum_{i=1}^{\infty} \pi r_i^2 C_i \ll 1 \tag{7}$$

If all clusters have the same radius, $r_i = r$, then $Z = (r/R)^2$, and eqn. (5) becomes identical to the result obtained from a lattice diffusion model [28].

In the other limiting case (desorption-controlled kinetics) which is typically encountered at high substrate temperatures, diffusion theory yields for an isolated circular cluster [2, 3]

$$\sigma_i = \frac{2\pi r_i}{\lambda} \frac{K_1(r_i/\lambda)}{K_0(r_i/\lambda)} \tag{8}$$

where λ is the diffusion length, $(D_1\tau)^{1/2}$, and K_0 and K_1 denote modified Bessel functions [31]. Except for very high temperatures where λ is only a few lattice constants, the expression in eqn. (8) may be approximated by [2, 3]

$$\sigma_i = 2\pi/\ln(\lambda/r_i) \tag{9}$$

Now consider the more general case where two moving clusters coalesce [expressed in eqn. (4)]. Since clusters do not evaporate, σ_{ij} may be given by an expression similar to eqn. (5),

$$\sigma_{ij} = 2\pi/\ln\left(\frac{R}{r_i + r_j}\right) \tag{10}$$

where $r_i + r_j$ is the distance of contact.

It must be emphasised that the expressions (5) and (9) are less rigorous than they might seem. This is mainly because the underlying diffusion theories do not take into account spatial correlations between clusters. Moreover, all these theories assume steady state, which is never strictly met in deposition experiments. The difficulties encountered in attempts to calculate rigorous coalescence-rate constants reveal, in fact, the limitations of the mean-field concept that is inherent in eqn. (1).

3.2. Models for cluster mobilities

The dominant size dependence of the coalescence rates is given by the diffusion coefficient, D_i [*cf.* eqn. (4)]. Monomer diffusion follows quite closely an Arrhenius relation [32],

$$D_1 = \tfrac{1}{4} a^2 \nu_1 e^{-E_1/kT} \tag{11}$$

where a is a hopping distance, ν_1 is the adatom vibration frequency, and E_1 is the activation energy for adatom diffusion. Furthermore, k is Boltzmann's constant and T is the surface absolute temperature.

The diffusion of clusters is much more complicated since different mechanisms with different activation energies are involved. In general, cluster diffusion does not obey a simple Arrhenius law [33]. The qualitative behavior depends on the relative bond strengths of the substrate and the deposit, and also on the mismatch in bond lengths.

In the one extreme, where the bonding between two adsorbate atoms is strong compared with the bonding between an adsorbate and a substrate atom, the cluster moves as a whole, and a relation

$$D_i \propto e^{-E_i/kT} \tag{12}$$

is suggested [3], where E_i is an energy proportional to the interface area. Clearly, the mobility decreases rapidly with increasing cluster size in this case.

In the other extreme where the internal bonds within a cluster are weak, cluster migration is thought to be caused by random self-diffusion of individual cluster atoms. Here, the diffusion coefficient obeys a power law [3]

$$D_i \propto i^{-s} \tag{13}$$

where the power exponent s depends on the dimensionality of the process. According to ref. 3, $s = 1$ corresponds to volume self-diffusion, $s = 4/3$ to surface self-diffusion, and $s = 5/3$ to peripheral self-diffusion.

It should be noted that eqns. (14) or (15) are based only on certain simplified theoretical models. Experimental information on cluster surface diffusion exists [5] but is scarce. It is interesting to note, however, that in some systems, dimers have been observed to have higher mobilities than monomers, which is incompatible with either eqn. (12) or eqn. (13). In this paper, we use the two mobility models represented by eqns. (12) and (13) to illustrate the possible range of mobility coalescence effects.

4. Calculations of size distributions

All our calculations are based on coalescence rates according to eqn. (4). However, in order to keep the number of parameters small, we used constant capture numbers, $\sigma_{ij} \equiv \sigma$. This is not a severe approximation since all the expressions given in section 3.1 have weak logarithmic dependence. At any rate, it is the diffusion coefficient rather than the capture number that contains the dominant size dependence in the coalescence rate.

To study the effects of cluster mobility on nucleation

kinetics, two different models are adopted. In the first model, dimers are assigned a certain fraction of the monomer mobility while all larger clusters are considered immobile. In the second model, mobilities are assumed to follow a power law according to eqn. (13). These two models allow a systematic study of mobility effects. Calculations with exponential size dependence as suggested by eqn. (12) were carried out as well [24], but the results are qualitatively the same as for the model where only dimers are mobile. Therefore, those calculations will not be reported here.

In nucleation theory, it is common to distinguish between two different regimes of condensation that are characterized by the relative importance of processes in the monomer balance (eqn. (2)). The first is the desorption-controlled case, where deposition and evaporation of adatoms are in equilibrium and aggregation can be neglected. In this case, eqn. (2) reduces to

$$C_1 = Q\tau \tag{14}$$

The second regime of condensation is the capture-controlled case, where loss due to aggregation dominates over evaporation. Here, eqn. (2) becomes

$$\frac{\partial}{\partial t}C_1 = -\sum_{j=1}^{\infty} K(1,j)C_1C_j + Q \tag{15}$$

We wish to keep this distinction here and discuss the effects of mobility coalescence for both extremes separately. The numerical solution of the system of clustering equations has been fully explored in ref. 24 and more detailed derivations can be found in ref. 30 [1]. For convenience, however, we summarize our numerical approach below.

A two-group method has been developed to solve the hierarchical system of eqns. (1) and (2). In this technique, small size clusters, up to an arbitrary size given by $i = x^*$, are obtained by a direct numerical solution to eqn. (1). Equations for the k's moment, M_k, of the size distribution have been derived, and are given by [24]:

$$\begin{aligned}\frac{\partial}{\partial t}M_k = &-\sum_{i=1}^{x^*} i^k \frac{\partial}{\partial t}C_i \\ &+\tfrac{1}{2}\sum_{i=1}^{x^*}\sum_{j=1}^{x^*} C_iC_jK(1,j)[(i+j)^k - i^k - j^k] \\ &+\sum_{i=1}^{x^*} C_i\int_{x^*}^{\infty} \mathrm{d}x C(x)K(1,x)[(i+x)^k - i^k - x^k] \\ &+\tfrac{1}{2}\int_{x^*}^{\infty}\int_{x^*}^{\infty} \mathrm{d}x\mathrm{d}y C(x)C(y)K(x,y) \\ &\times[(x+y)^k - x^k - y^k] + \sum_{i=1}^{\infty} i^k Q_i\end{aligned} \tag{16}$$

Instead of solving a large hierarchy of clustering equations (e.g. thousands) of the type represented by eqn. (1), a small number of kinetic moment equations (eqn. 16)) are solved. The solution for the discrete group is appropriately attached to the moment at $i = x^*$. The size distribution is then reconstructed from the moments by a modification of the maximum entropy principle [34, 35] as explained in ref. 24.

4.1. Desorption-controlled case

The number of parameters may be reduced without loss of generality by appropriately rescaling quantities,

$$C_i' = C_i/(Q\tau)$$

$$t' = \sigma D_1 Q\tau t \tag{17}$$

This transformation removes Q, τ, σ, and D_1 from the calculations. The only input parameters left is the ratio of the diffusion coefficients, D_i/D_1. All results in this section will be given in terms of the dimensionless primed quantities. Table 1 gives the magnitude of input parameters used in example calculations. The values of the parameters in Table 1 are chosen to illustrate a typical high-temperature deposition case.

TABLE 1. Input model parameters "Illustrative example"

Symbol	Parameter meaning	Value	Units
D_1	monomer diffusion coefficient	10^{-10}	$m^2\ s^{-1}$
τ	mean adatom residence time	10^{-8}	s
Q	monomer deposition rate	10^{17}	$m^{-2}\ s^{-1}$

In this example, all C_i's will denote concentrations in units of $10^9\ m^{-2}$, and t will be the time in units of 10 s.

Figure 1(a) shows the time dependence of the concentrations of the five smallest clusters together with the zeroth moment, M_0 of all larger clusters:

$$M_0 = \sum_{i=6}^{\infty} C_i \tag{18}$$

Only monomers are assumed to be mobile. Initially, atoms are present on the substrate surface at their equilibrium concentration (eqn. (14)), while all other concentrations are set equal to zero. As time proceeds, dimers and larger clusters are formed until they reach a common "quasi-equilibrium" value. We define here "quasi-equilibrium" as the condition which exists when $C_2 = C_3 = C_4 \ldots$ Here, the gain of i-clusters by monomer aggregation to $(i-1)$-clusters is compensated for by an equal loss due to monomer aggregation to i-clusters. The zeroth moment of clusters with six or more atoms increases linearly because six-mers are produced at a constant rate.

Figure 1(b) shows the same results except that dimers have finite mobility, $D_2 = D_1/100$. The behavior in the initial stage is identical with the behavior shown in

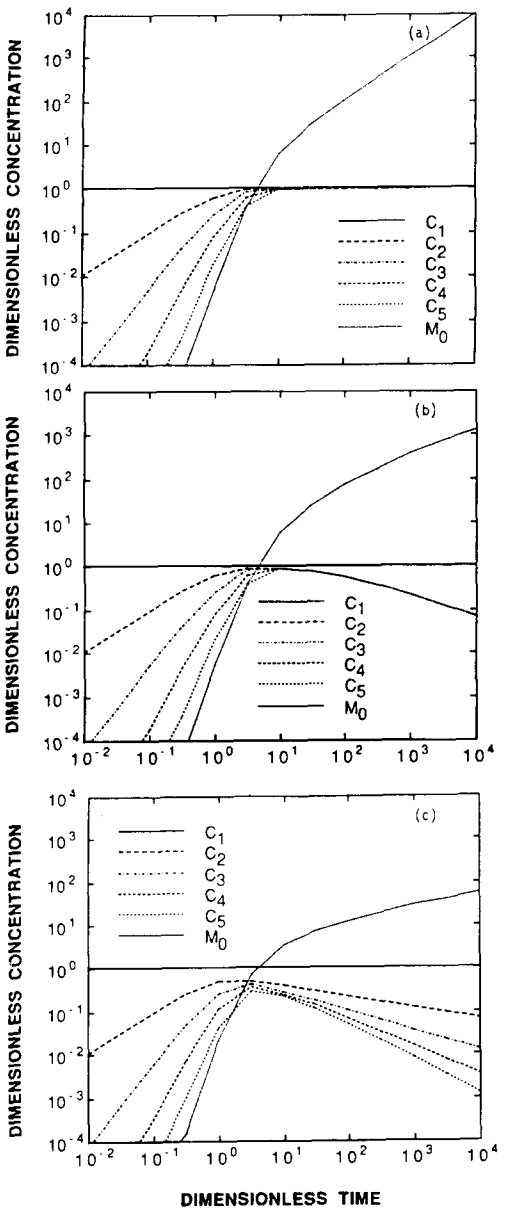

Fig. 1. Time dependence of small cluster concentrations $C_1 \ldots C_5$, and of the zeroth moment (M_0) for the desorption-controlled case: (a) monomers mobile only, (b) dimers mobile with $D_2 = D_1/100$; (c) all clusters mobile (eqn. (15) with $s = 2$). (The quantities are made dimensionless according to eqn. (17).)

Fig. 1(a), but for $t' > 10$ there is a marked difference. The concentrations of dimers and larger clusters pass through a maximum, followed by a continuous decrease. Here, dimers are lost because of aggregation to other clusters. Consequently, all concentrations of larger clusters decrease as well, and the zeroth moment of clusters with six or more atoms increases sub-linearly. It is remarkable that this effect is present even for such a low dimer mobility of 1%.

Figure 1(c) displays the evolution of concentrations where all clusters are mobile according to a power law (eqn. (13) with $s = 2$). The initial phase is the same as in the previous figures since coalescence does not operate before sufficient cluster concentrations have built up. However, after passing through a maximum, the concentrations do not assume common quasi-equilibrium values since clusters of any size are lost by aggregation to larger ones. Therefore, the total production rate (for clusters of size $i \geq 3$) is reduced because of the loss of dimer growth centers.

Figure 2(a) shows size distributions for a fixed time, $t' = 1000$. The different curves correspond to different dimer mobilities. The solid line, representing zero dimer mobility, shows features of a propagating step function (*i.e.* clusters with less than 1000 atoms occur with concentrations around unity, where larger clusters are practically absent). The waviness of the distribution for $i \leq 1000$ in the case when dimers are immobile (solid lines) is not real but is an artifact of our method of solution that is caused by the reconstruction of the distribution from its moments [24]. The accuracy of the reconstruction is substantially improved in cases where dimers are mobile (dashed lines). A complete analysis of the numerical problems associated with reconstructing

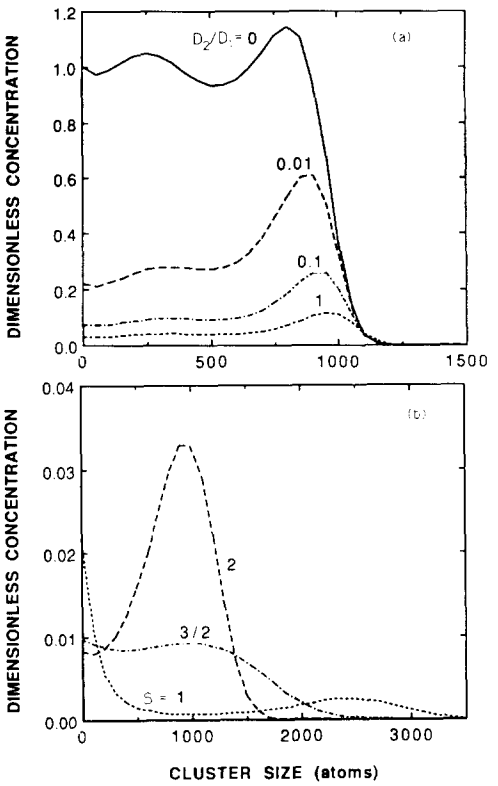

Fig. 2. Cluster-size distribution function for the desorption-controlled case, at dimensionless time $t' = 1000$: (a) dimers are mobile with their diffusion coefficient indicated as a fraction of the single atom value (reconstructed from five moments), (b) all clusters are mobile with mobility size-dependence given by the various values of the power s (eqn. (13)) (reconstructed from three moments).

the distribution function from a small number of moments is given by us in refs. 24 and 30. The broken curves in Fig. 2 (a) show size distributions for finite dimer mobility. All distributions have the same qualitative behavior (*i.e.* the concentrations increase with increasing size, followed by a pronounced maximum and a sharp drop-off at around $i = 1000$). The exact position of the maximum concentration shifts to larger sizes as the mobility of dimers increases. This is to be expected if an increasing proportion of dimers contribute to cluster growth through capture. This implies that dimer mobility does not significantly enhance the growth rate of existing clusters, as one might expect. Rather, dimer mobility results in a loss of dimer growth centers and thus reduces the rate of formation of higher-order clusters. Therefore, all broken curves in Fig. 2(a) fall below the solid curve.

The situation is more complex for the distributions in Fig. 2(b), where power-law mobility (eqn. (15)) is assumed with various powers s. As in Fig. 2(a), mobility is found to decrease the total number of clusters per unit area, *i.e.* the integral over the distribution. Unlike Fig. 2(a), however, the growth rate increases with an increasing degree of cluster mobility, *i.e.* decreasing s. Whereas the maximum of the distribution is around $i = 1000$ for $s = 2$, it is at around $i = 2500$ for $s = 1$. Also the shape of the distribution seems to depend qualitatively on the power exponent s. While for $s = 2$, the bulk of the distribution is made up of larger clusters of sizes around $i = 1000$, there is a comparatively large fraction of small clusters for $s = 1$. This may be explained by the fact that for $s = 1$ there are fewer clusters than for $s = 2$, thus resulting in a smaller chance for the small clusters to aggregate to large ones. Hence, more of them survive, as is seen in the distribution function.

4.2. Capture-controlled case

In this section we rescale quantities according to

$$C_i' = (\sigma D_1/Q)^{1/2} C_i$$

$$t' = (\sigma D_1 Q)^{1/2} t \qquad (19)$$

This makes the quantities σD_1 and Q disappear from both eqns. (1) and (15), and the behaviour of the system is completely determined by the relative cluster diffusion coefficients, D_i/D_1. As an example, one may consider quantities which are representative of low-temperature condensation. If the values of $D_1 = 10^{-13}$ m^2 s^{-1}, $Q = 10^{19}$ m^{-2} s^{-1} were used, the C_i's will denote concentrations in units of 10^{16} m^{-2} and t' will be the time in units of 10^{-3} s.

Figure 3(a) shows the time dependence of individual dimensionless concentrations. Here, the monomer concentration is not constant but is determined by the balance of eqn. (15). At short times, C_1 increases linearly because there is a constant source Q and essentially no loss by aggregation. For $t' > 1$, however, aggregation sets in, and the adatom concentration decreases [1] as $C_1 \propto 1/t^{1/3}$. Quasi-equilibrium is achieved for all displayed concentrations at times $t' > 10$ (*i.e.* all concentrations are equal to C_1). The zeroth moment of large clusters increases as $M_0 \propto t^{1/3}$ for sufficiently long times [1].

Figure 3(b) depicts the same set of parameters but with dimer mobility $D_2 = D_1/100$. Here the dimer concentr-

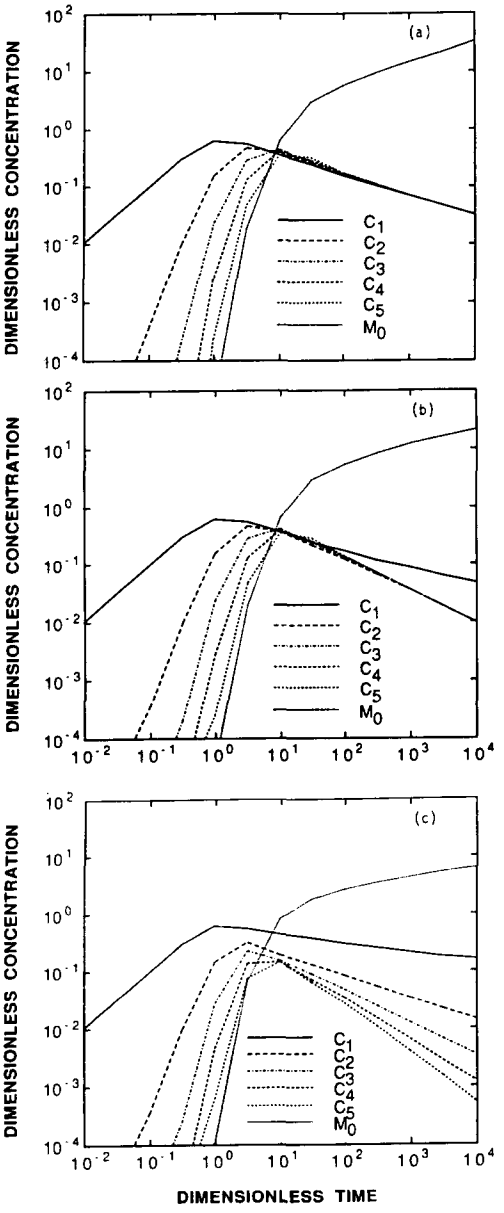

Fig. 3. Time dependence of small cluster concentrations $C_1 \ldots C_5$, and of the zeroth moment (M_0) for the capture-controlled case: (a) monomers mobile only, (b) dimers mobile with $D_2 = D_1/100$, (c) all clusters mobile (eqn. (15) with $s = 2$). (The quantities are made dimensionless according to eqn. (19).)

ation decreases more rapidly at long times compared with the case where dimers are not mobile (Fig. 3(a)). Here, nucleation centers are lost, resulting in a smaller total zeroth moment of large clusters. This has a feedback effect on adatoms in that they have fewer partners to aggregate with and, thus, remain more abundant in comparison to the previous case of Fig. 3(a) where dimers are not mobile. The abundance of adatoms, in turn, has implications on the growth rate, as will be shown below.

Figure 3(c) shows the evolution of concentrations for power-law mobility [eqn. (13) with $s = 2$]. There is no quasi-equilibrium for long times since clusters of any size may be lost due to aggregation. The formation of large clusters is much slower than in the previous figures because the independence of clusters is lost while they are still small. Compared with Figs. 3(a) and 3(b), more monomers survive because they meet fewer large clusters with which to aggregate.

Size distributions for different dimer mobilities are shown in Fig. 4(a). It is seen that with increasing dimer mobility (shown as a fraction of the monomer mobility on the curves), the total number of clusters decreases. On the other hand, the growth rate increases with increasing dimer mobility. The reason here is not, as might be suspected, that clusters grow to a noticeable degree by dimer aggregation [monomer aggregation is the dominant growth mechanism for all cases displayed in Fig. 4(a)]. Rather, the increase in growth rate is caused by an increased monomer concentration for increased dimer mobility, as can be seen by comparing Figs. 3(a) and 3(b).

Finally, size distributions for power-law mobility with various exponents s are shown in Fig. 4(b). Apart from the different scale, there is a striking similarity to the curves in Fig. 2(b). This behavior suggests that for power-law mobility, the shape of the distribution is not dependent on the details of the monomer balance. This is in contrast to the case where only monomers are mobile (where the size distribution is a "mirror image" of the temporal monomer concentration [1]).

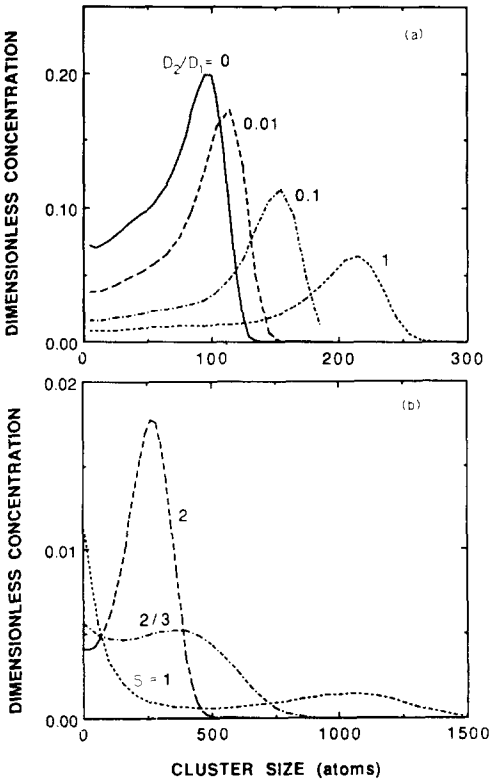

Fig. 4. Cluster-size distribution functions for the capture-controlled case, at dimensionless time $t' = 1000$: (a) dimers are mobile with their diffusion coefficient indicated as a fraction of the single atom value (reconstructed from five moments), (b) all clusters are mobile with various values for s shown on the curves (eqn. (13)) (reconstructed from three moments).

5. Conclusions

We have presented a kinetic study of mobility effects on cluster evolution during the deposition of atoms onto a surface. Calculations have been carried out for two extreme regimes of condensation: the capture-controlled and the desorption-controlled cases. Cluster mobility has been modeled either as dimer mobility only or as a power-law dependence where even large clusters are fairly mobile.

Our results suggest the following conclusions:

(1) If only monomers are mobile, the size distribution is essentially a mirror image of the time dependence of the monomer concentration [1]. This simple picture is valid if all clusters grow in a deterministic fashion (fluctuations due to the discreteness of the aggregation process being negligible).

(2) Dimer mobility causes dimer depletion due to aggregation with larger clusters. Consequently, since they grow from dimers, the concentrations of trimers and all larger clusters are depleted also. The size distribution is a mirror image of the dimer concentration as a function of time. Cluster growth is still dominated by single atom aggregation.

(3) The case where large clusters are mobile is more complex. For a power-like dependence of cluster mobility, clusters grow to a certain degree by cluster aggregation in addition to single particle aggregation. The size distribution no longer reflects the time dependence of monomers or even small clusters. Typical size distributions display a sharp decrease at small sizes and a peak at large sizes. Our numerical results are consistent with the qualitative arguments of Venables and Bienfait [36], and Venables *et al.* [6].

Acknowledgment

This work has been made possible by a fellowship from the science committee of NATO, administered by the German Academic Exchange Service (DAAD).

References

1 G. Zinsmeister, *Thin Solid Films, 2* (1968) 497; *4* (1969) 363.
2 J. A. Venables, *Philos. Mag., 27* (1973) 697.
3 B. Lewis and J. C. Anderson, *Nucleation and Growth of Thin Films*, Academic, New York, 1978.
4 H. Schmeisser, *Thin Solid Films, 22* (1974) 83.
5 D. W. Bassett, in V. T. Binh (ed.), *Surface Mobilities on Solid Materials*, Plenum, New York, 1983, pp. 63–108.
6 J. A. Venables, G. D. T. Spiller and M. Hanbücken, *Rep. Prog. Phys., 47* (1984) 399.
7 J. A. Adams and W. N. G. Hitchon, *J. Comput. Phys., 76* (1988) 159.
8 H. D. Velfe and M. Krohn, *Thin Solid Films, 98* (1982) 125.
9 G. A. Bassett, *Proc. Eur. Reg. Conf. Electron Microscopy*, Vol. 1, North Holland, Amsterdam, 1961, p. 220.
10 G. A. Bassett, in E. Rutner, P. Goldfinger and J. P. Hirth (eds.), *Proc. Int. Symp. Condensed Evaporated Solids*, Gordon and Breach, New York, 1964, p. 599.
11 H. Poppa, *J. Appl. Phys., 38* (1967) 3882.
12 D. B. Dove, *J. Appl. Phys., 35* (1964) 2784.
13 L. Bachman, D. C. Sawyer and B. C. Siegel, *J. Appl. Phys., 36* (1965) 304.
14 J. G. Skofronick and W. B. Philips, *J. Appl. Phys., 38* (1967) 4791.
15 A. Masson, J. J. Metois and R. Kern, *Surf. Sci., 27* (1971) 283.
16 U. Schwabe and K. Hayek, *Thin Solid Films, 12* (1972) 403.
17 J. C. Zanghi, J. J. Metois and R. Kern, *Philos. Mag., 31* (1975) 743.
18 K. Heinemann and H. Poppa, *Thin Solid Films, 33* (1976) 237.
19 M. V. Smoluchowski, *Physik. Z., 17* (1916) 557.
20 S. K. Friedlander, *Smoke, Dust and Haze*, Wiley-Interscience, New York, 1977.
21 G. B. Field and W. C. Saslaw, *Astrophys. J., 142* (1965) 568.
22 S. Chandrasekhar, *Rev. Mod. Phys., 15* (1943) 1.
23 Z. A. Melzak, *Trans. Am. Math. Soc., 85* (1957) 547.
24 M. Vicanek and N. M. Ghoniem, *Two-Group Approach to the Kinetics of Particle Cluster Aggregation*, University of Los Angeles report UCLA-ENG-9026/PPG-1328, 1990 *J. Comput. Phys.*, in the press.
25 A. D. Gates and J. I. Robins, *Thin Solid Films, 149* (1987) 113.
26 C. A. Stone and N. Ghoniem, *J. Vac. Sci. Technol., A9* (3) (1991) 759.
27 R. Fastenau, Ph.D. Thesis, Technical Highschool Delft, Netherlands, 1982.
28 M. J. Stowell, *Philos. Mag., 26* (1972) 349.
29 B. Lewis and G. J. Rees, *Philos. Mag., 29* (1974) 1253.
30 M. Vicanek, *Derivations and Solution Methods of Evolution Equations for Surface Atomic Clustering*, University of Los Angeles report UCLA-ENG-9025/PPG-1321, August 1990 [can be obtained from one of the authors on request].
31 F. W. J. Oliver, in M. Abramowitz and I. A. Stegun (eds.), *Handbook of Mathematical Functions*, National Bureau of Standards, Washington DC, 1965, pp. 355.
32 R. Gomer, in V. T. Bihn (ed.), *Surface Mobilities on Solid State Materials*, Plenum, New York, 1983, p. 7.
33 S. Stoyanov and D. Kashiev, in E. Kaldis (ed.), *Current Topics in Materials Science, Vol. 7*, North-Holland, Amsterdam, 1981, p. 69.
34 E. T. Jaynes, in D. W. McLaughlin (ed.), *Inverse Problems*, Am. Math. Soc. Providence, RI, 1984, p. 151.
35 W. T. Grandy, Jr., in C. Ray Smith and W. T. Grandy, Jr., (eds.), *Maximum Entropy and Bayesian Methods in Inverse Problems*, Reidel, Dordrecht, 1985, p. 1.
36 J. A. Venables and M. Bienfait, *Surf. Sci., 61* (1976) 667.